Transparent Fused Nanowire Electrodes by Condensation Coefficient Modulation

ADVANCED FUNCTIONAL MATERIALS
www.afm-journal.de

Transparent Fused Nanowire Electrodes by Condensation Coefficient Modulation

*Jaemin Lee, Silvia Varagnolo, Marc Walker, and Ross A. Hatton**

Silver nanowire networks can offer exceptionally high performance as transparent electrodes for stretchable sensors, flexible optoelectronics, and energy harvesting devices. However, this type of electrode suffers from the triple drawbacks of complexity of fabrication, instability of the nanowire junctions, and high surface roughness, which limit electrode performance and utility. Here, a new concept in the fabrication of silver nanowire electrodes is reported that simultaneously addresses all three of these drawbacks, based on an electrospun nanofiber network and supporting substrate having silver vapor condensation coefficients of one and near-zero, respectively. Consequently, when the whole substrate is exposed to silver vapor by simple thermal evaporation, metal selectively deposits onto the nanofiber network. The advantage of this approach is the simplicity, since there is no mask, chemical or dry metal etching step, or mesh transfer step. Additionally, the contact resistance between nanowires is zero and the surface roughness is sufficiently low for integration into organic photovoltaic devices. This new concept opens the door to continuous roll-to-roll fabrication of high-performance fused silver nanowire electrodes for myriad potential applications.

1. Introduction

Electrospun polymer nanofibers (NFs) are versatile materials for the fabrication of transparent metal nano-network (NN) electrodes and stretchable metal meshes[1–8] for use in a variety of applications including transparent heaters,[6] organic photovoltaics (OPVs),[1] organic light-emitting diodes,[7] and wearable electronics.[8] The NFs can be used to fabricate metal nano-network electrodes in two different ways: i) Bottom-up approaches in which an electrospun polymer NF network serves as a seed for electroless plating or vacuum deposition of metal, followed by selectively transferring the metallized polymer network to another substrate;[2,8,9] or ii) top-down approaches in which a polymer NF network is spun onto a thin metal film where it serves as a metal etch mask.[1,4,7] After etching away the metal area not covered with polymer NFs, the NFs themselves are removed to reveal a network of metal lines with uniform height and zero-junction resistance making them suitable for use in thin film electronics.[1,7] Junction-free nano-networks are highly desirable because the contacts between separate metal wires are susceptible to oxidation and localized heating[10] which is the Achilles' heel of nano-network electrodes based on separate metal nanowires. To the best of our knowledge, to date only nano-network electrodes fabricated using the top-down approach have proved suitable as the substrate electrode in efficient OPVs, since electrodes fabricated using bottom-up approaches have too high, or uncontrollable surface roughness, which results in electrical losses due to shunting across the thin organic semiconductor layers used in this important class of emerging photovoltaic device.[1]

Here, we report a new scalable approach to the fabrication of junction-free, high-performance transparent silver (Ag) nanowire network electrodes which completely avoids the need for a complex metal nano-network transfer step or metal etching step, thereby greatly simplifying the process of electrode fabrication. This unconventional approach to fabrication of this important class of transparent electrode exploits the fact that highly fluorinated organic compounds can exhibit an extremely small condensation coefficient for Ag vapor[11] and uses a NF composition of electrospun nanowires that enables junction-free contacts between nanowires to be achieved. Transparent Ag electrodes with an average transparency of 90.8% across the wavelength range 400–800 nm and a sheet resistance of 6.3 Ω sq^{-1} are fabricated using this method, and their utility is demonstrated as transparent, flexible heaters and transparent substrate electrodes for solution processed OPVs.

2. Results and Discussion

The new simplified approach to metal nano-network fabrication is schematically illustrated in **Figure 1**. Polyvinylpyrrolidone

Dr. J. Lee,[+] Dr. S. Varagnolo,[++] Prof. R. A. Hatton
Department of Chemistry
University of Warwick
Coventry CV4 7AL, UK
E-mail: Ross.Hatton@warwick.ac.uk
Dr. M. Walker
Department of Physics
University of Warwick
Coventry CV4 7AL, UK
The ORCID identification number(s) for the author(s) of this article can be found under https://doi.org/10.1002/adfm.202005959.

[+]Present address: School of Mechanical Engineering, University of Leeds, Leeds LS2 9JT, UK
[++]Present address: School of Engineering and Innovation, The Open University, Milton Keynes MK7 6AA, UK

DOI: 10.1002/adfm.202005959

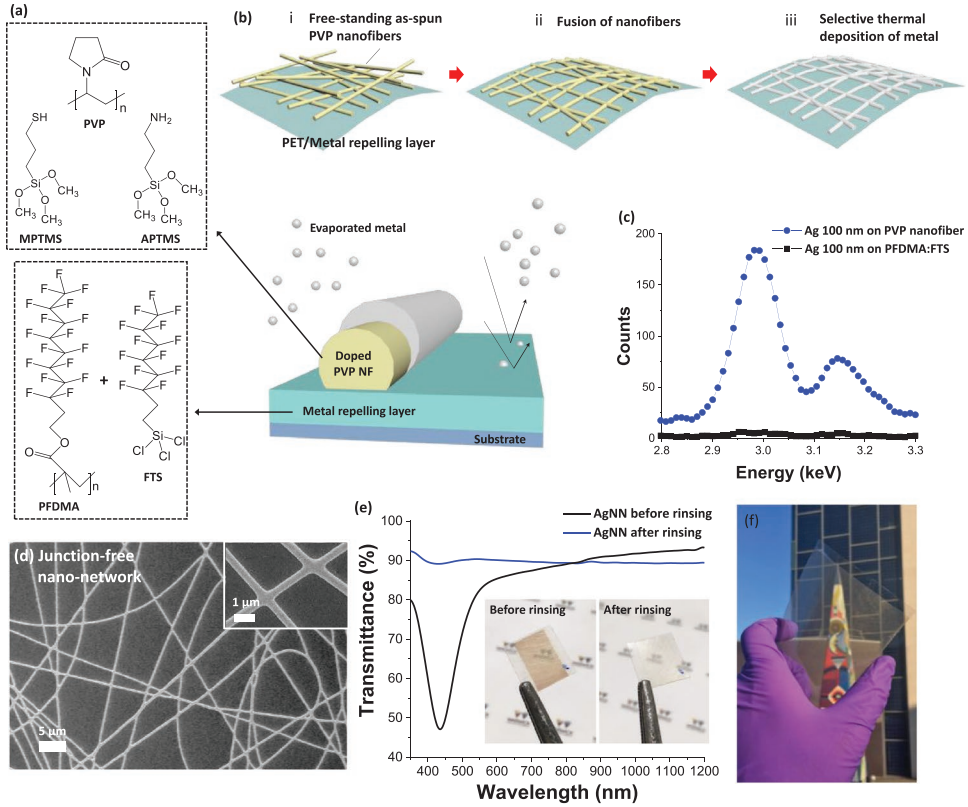

Figure 1. a) Schematic of methoxysilane doped PVP nanofibers (NFs) and the underlying silver repelling layer composed of a blend of FTS and PFDMA; b) illustration of the stages of metal nano-network (NN) fabrication: free-standing electrospun NFs (i) are fused (ii) and metal is selectively deposited onto the fused NFs network (iii) by condensation coefficient modulation.; c) EDX analysis of the doped PVP NFs and PFDMA:FTS metal repelling layer, from which the condensation coefficients are determined; d) SEM image of the fused Ag nano-network electrode: Inset showing a magnified image from the same network. The average diameter of Ag nanowires is ≈430 nm.; e) total transmittance of the Ag nano-network before and after rinsing with HFE-7500 for 10 s. These images clearly show that the small amount of Ag in the gap between nanowires can be easily removed; f) an 8 cm × 8 cm large-area Ag nano-network electrode on PET.

(PVP) nanowires doped with 3-mercaptopropyl trimethoxysilane (MPTMS) and 3-aminopropyl trimethoxysilane (APTMS) (Figure 1a) are electrospun directly onto flexible plastic substrates coated with a thin film of an organofluorine polymer-small molecule blend: poly(3,3,4,4,5,5,6,6,7,7,8,8,9,9,10,10,10-heptadecafluorodecyl methacrylate) (PFDMA):trichloro(1H,1H,2H,2H-perfluorooctyl)silane (FTS) (Figure 1a,b(i)). The diameter of the PVP nanowires was 294 nm ± 47 nm before metallization. The nanowires then undergo a facile fusion step (Figure 1b(ii)) which also serves to reduce the surface roughness before exposing the whole substrate to metal vapor in a conventional vacuum evaporator, whereupon 100 nm Ag film selectively condenses onto the doped polymer NFs wires, forming junction-free metal nano-networks (Figure 1b(iii)).

We have recently reported that a printed layer of FTS (Figure 1a) can have a near-zero condensation coefficient for Ag vapor when its thickness is greater than 10 nm, and so FTS can be used to fabricate patterned Ag films by condensation coefficient modulation.[11] However, the intermolecular attractive forces in organofluorines are exceptionally weak, due to the low polarizability of the carbon—fluorine bond together with the relatively large intermolecular separation that results from steric repulsion between fluorine atoms. Consequently, in general, organofluorines exhibit very low surface tension and solutions of small molecule organofluorines such as FTS have a very low viscosity, making it difficult to form uniform thin films of controllable thickness above 10 nm. For this reason, in the current context, we have combined FTS with PFDMA (Figure 1a) to make a PFDMA:FTS blend with a very low condensation coefficient for Ag that is easily cast into thin films with tuneable thickness onto a variety of substrates. This organofluorine blend was coated onto a flexible polyethylene terephthalate (PET) substrate to a thickness of 130 nm, well above the critical thickness of 10 nm. NFs of PVP doped with the bifunctional small molecules, MPTMS and APTMS (APTMS:MPTMS = 1:1, 1.67 wt%), were then electrospun directly onto the organofluorine layer (Figure 1b). The rationale for the inclusion of these trimethoxysilane additives is twofold: i) they are able to cross-link when hydrolyzed, a reaction that is catalyzed by the primary amine on APTMS,[12] forming a network of strong siloxane linkages which helps to improve the mechanical strength of the PVP matrix; ii) the thiol moiety on MPTMS binds strongly with Ag,[13] improving the strength of adhesion between the metal film and the NFs and so improving the thermal and mechanical durability.

As is typical for electrospun polymer NFs, the as-spun NFs are not fused together and some parts are suspended above the substrate (Figure S1, Supporting Information). To fuse the NFs, the NF network was cooled to 5 °C in a fridge for 10 min and

then exposed to room temperature air at 50% relative humidity (Figures S1 and S2, Supporting Information). This simple process enables sufficient water to condense onto the NFs to soften them so that they fuse, while also providing water to promote the cross-linking reaction between the methoxysilane additives.[14] The whole substrate was then exposed to Ag vapor in a vacuum evaporator until a total thickness of 100 nm had deposited onto a quartz crystal microbalance adjacent to the substrate. Spatially resolved energy-dispersive X-ray spectroscopy (EDX) analysis (Figure 1c) shows that the condensation coefficient for Ag onto the doped PVP NFs is 1.0, while on the organofluorine regions it is ≤0.05. Consequently, a continuous 100 nm thick nanowire network is formed with fused contacts between wire intersection points (Figure 1d), and only a tiny amount of Ag is deposited in the gaps between NFs. The conducting atomic force microscope (C-AFM) mapping in **Figure 2** shows no evidence for higher resistance (i.e., reduced current) at the nanowire intersection points, consistent with junction-free contacts. The AFM and secondary electron microscope (SEM) images in Figures S3 and S4, Supporting Information also show that the width-to-height ratio of the metallized NFs is greater than 2.5:1, which indicates that the NFs are not only fused as a result of water vapor treatment step, but also flattened, which is beneficial for subsequent application in OPVs.

For 100 nm Ag deposited onto the doped NF network, the EDX analysis (Figure 1c) shows that ≤5 nm is deposited onto the adjacent organofluorine regions. At such low effective thickness, the Ag forms nanoparticles which are well known to couple strongly with the incident light in the blue part of the spectrum due to excitation of localized surface plasmon resonant excitations.[15] Consequently, immediately after Ag deposition, the metal nano-network has a brown tinge (Figure 1e, inset and Figure S5, Supporting Information), although this coloration is easily removed either by briefly rinsing the electrode in fluorinated solvent (HFE-7500) which removes the top 35–40% of the organofluorine layer or by a brief UV-O_3 treatment, neither of which negatively affect the electrode sheet resistance when performed for the optimal time (Figure S5, Supporting Information). Notably, the brown tinge is not easily removed when the organofluorine layer is PFDMA only (Figure S5, Supporting Information) and so the inclusion of FTS is critical for the efficacy of this step. Whilst the underlying reason for this is not yet fully understood, it is tentatively suggested that the FTS phase separates to the surface of the blend film and is more easily removed by solvent rinsing due to its lower molecular weight. To show that this fabrication method can be applied to a larger area, we have fabricated an 8 cm × 8 cm electrode on PET (Figure 1f).

The correlation between total far-field transparency (specular and diffuse) and sheet resistance of the Ag nano-networks is shown in Figure 2c together with that of nanowire network electrodes reported in the literature.[1,2,16,17] It is evident that all of the Ag nanowire networks fabricated using our method have a direct current conductivity/optical conductivity (σ_{DC}/σ_{Op}) between 600 and 800, which fulfils the industrial requirements

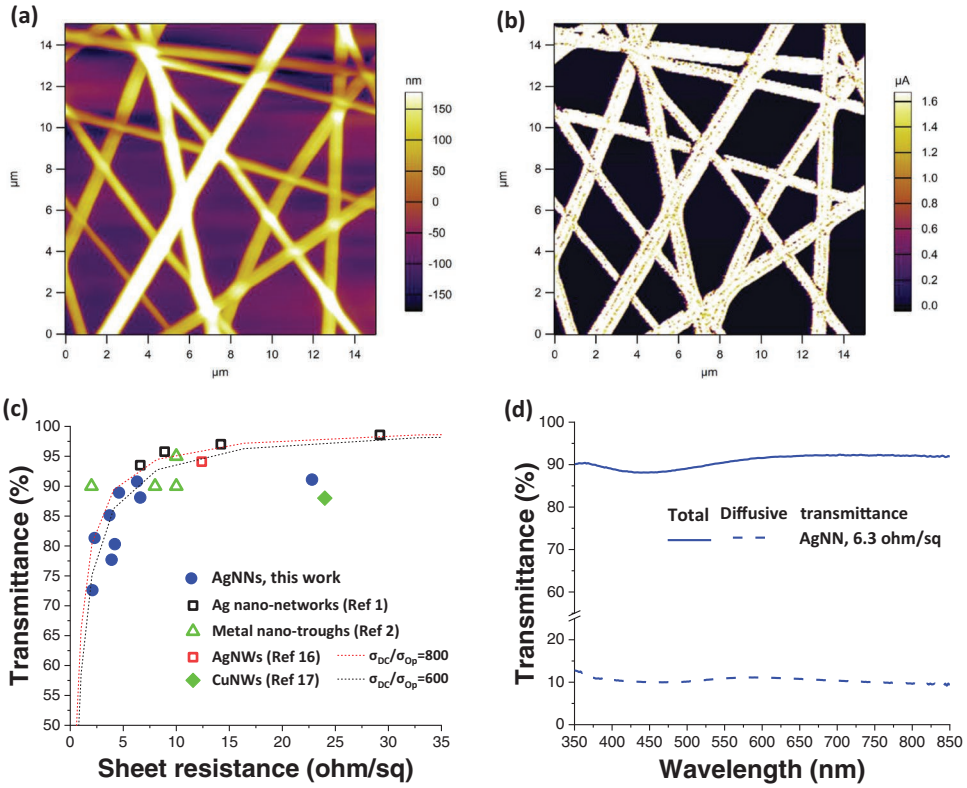

Figure 2. Morphological and opto-electrical characteristics of silver nano-networks on flexible PET substrates following brief rinsing with the fluorinated solvent (HFE-7500). a) Morphology and b) current mapping measured using an AFM in tapping mode and conductance mode, respectively; c) average far-field transmittance over wavelength range 400–800 nm versus sheet resistance of various Ag nano-network electrodes fabricated in this study together with other ITO-alternatives reported in the literature; d) total and diffusive (scattered) transmittance of the optimized Ag nano-network electrode.

of 85% transmittance at 10–15 Ω sq^{-1} sheet resistance for photovoltaic applications and displays.[1,18] For a total transparency of 90.8%, the electrode sheet resistance is 6.3 Ω sq^{-1}, performance that is comparable to the best reported for metal nanowire electrodes fabricated using conventional top-down etching methods.[1,4,7] The relatively large diffuse contribution to the transparency, ≈10%, in Figure 2d is expected given the narrow width of the Ag nanowires (≈430 nm), and is an advantage for thin film photovoltaics applications, since forward light scattering helps to ensure light remains trapped in the device.

Indirect evidence for the important role played by the methoxysilane additives in the PVP NFs is provided by the improved thermal and mechanical stability of the Ag nanowire network (**Figure 3**). When heated to 150 °C, which corresponds to the melting point of PVP, the nanowire networks with and without silane additives exhibit negligible change in sheet resistance. However, when the temperature is increased to 200 °C only nanowire networks fabricated on methoxysilane doped PVP are stable (Figure 3a). SEM imaging reveals that the sheet resistance of networks without silane doping in the PVP increases due to the formation of disconnects in the metal networks (Figure S6, Supporting Information). It is well known that molecules bearing trimethoxysilane moieties, such as APTMS and MPTMS can cross-link when hydrolyzed forming stable Si—O—Si bonded networks.[14] In the current context, such cross-linking would be expected to improve the thermal and mechanical stability of PVP NFs. Direct evidence for methoxysilane cross-linking is provided by X-ray photoelectron spectroscopy analysis (XPS) of doped PVP NFs (Figure S7, Supporting Information).

To test the stability of the fused nanowire electrodes on PET toward mechanical strain, they were bent 100 times with 3, 4, and 5 mm bending radii (Figure 3b and Figure S8, Supporting Information). Also shown in Figure 3b is the performance of commercial transparent electrodes based on ITO coated PEN, to demonstrate the poor compatibility of conventional transparent conducting oxides with flexible plastic substrates. For a 4 mm bending radius, cracks form in the ITO film after only a few bending cycles, whereas the Ag nanowire films are stable even with narrower film bending radius. Ag nanowire networks were also fabricated on a polydimethylsiloxane (PDMS) elastomer film in place of PET, and the resistance change ($\Delta R/R_0$) was measured under tensile strain (Figure 3c). For nanowire networks fabricated using silane doped PVP, the $\Delta R/R_0$ is 28 at 80% strain, which increases to 112 for nanowire networks fabricated without silane additives in the PVP. Close inspection of the strained nanowire networks reveals cracks have formed in the underlying organofluorine layer, and Ag nanowires without silane in the underlying PVP tend to fracture at these stress points even at as little as 30% strain (Figure 3d). Conversely, nanowires with MPTMS:APTMS in the PVP are much

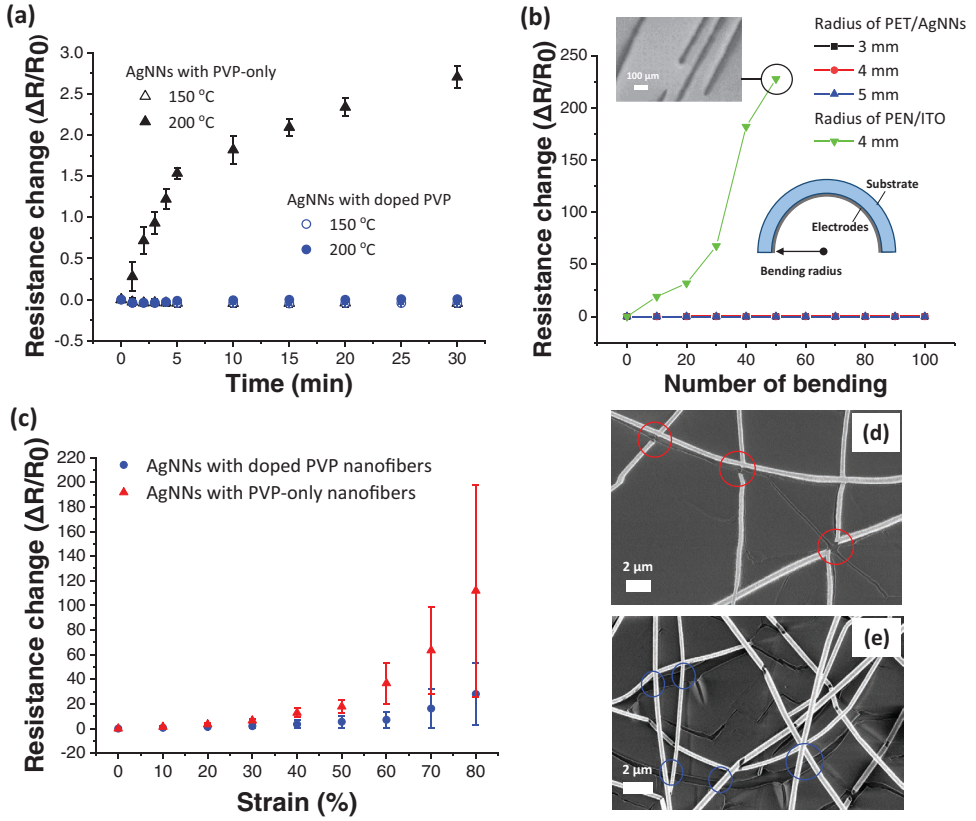

Figure 3. Thermal and mechanical durability testing of Ag nano-network electrodes: a) thermal stability of electrodes with and without APTMS and MPTMS additives in electrospun PVP nanofibers; b) bending test with different bending radii for Ag nano-network electrodes and 4 mm bending radius for PEN/ITO electrodes. Inset is an SEM image showing cracks in the ITO on PEN after bending; c) stretching test of Ag nano-network supported on a 60 µm thick polydimethylsiloxane (PDMS) substrate, with and without methoxysilane doping in the PVP nanofibers. SEM images of Ag nano-network on PDMS with undoped PVP nanofibers when stretched with 30% strain (d) and methoxysilane doped PVP nanofibers when stretched with 50% strain (e).

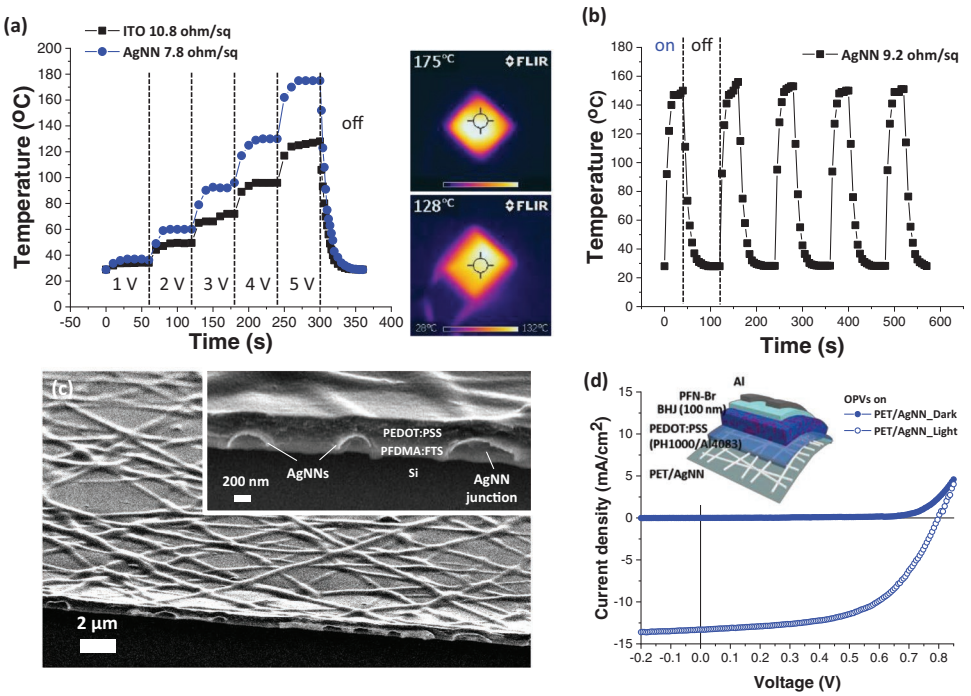

Figure 4. Transparent heater and OPV device demonstrations: a) performance of flexible PET/Ag nano-network (NN) and PEN/ITO transparent heaters at 1–5 V bias. Also shown are thermal camera images of PET/Ag nano-network (top right) and PEN/ITO (bottom right) at 5 V applied potential; b) on–off heating cycle response for PET/Ag nano-network; c) SEM image (70° tilted) of Si wafer/PFDMA:FTS/Ag nano-network/PEDOT:PSS showing conformal coating by PEDOT:PSS; d) current–voltage characteristic of a model OPV device tested in the dark and under 1 sun simulated solar illumination using the Ag nano-network on PET as a substrate electrode, together with a schematic of the device architecture.

more resistant to fracturing and tend to delaminate before fracturing (Figure 3e and Figure S9, Supporting Information). Furthermore, when the electrode on PET is intensively rinsed with fluorinated solvent HFE-7500 for an extended period, it becomes possible to transfer the metal network onto a PDMS substrate (Figure S10, Supporting Information). Crucially this operation can be performed with negligible change in the sheet resistance of the nanowire network (Figure S10, Supporting Information), which is further evidence of its mechanical robustness of the Ag network.

To demonstrate application of these fused nanowire electrodes, we have tested their potential as flexible transparent heaters, as compared to ITO on PEN (**Figure 4**a and Figure S11, Supporting Information). As shown in Figure 4a, the Ag nanowire heats up at lower applied voltage than ITO, well below the typical operating voltage required for window heaters used in commercial automobiles of 12 V.[19,20] Additionally, the temperature of the nanowire network stabilizes more quickly than ITO and exhibits a uniform heat distribution (top right) at 5 V bias even upon bending. The sub-micron diameter of our nanonetworks leaves scope for a high degree of freedom for control of nanowire density, enabling uniform heat distribution.

It is well known that for OPV devices to realize their full functional advantages (i.e., flexibility and light weight) and cost advantage over thin film photovoltaic devices, a high performance, low cost flexible transparent substrate electrode is needed.[21] Until now, bottom-up approaches to the fabrication of electrospun nanowire electrodes have yielded looks like that are too rough to be suitable for utility in thin class of device. Due to the combination of narrow nanowire diameter and the flattened, fused morphology of the nanowire networks fabricated using the method reported herein, they are suitable as transparent substrate electrodes in OPV devices with a photoactive layer thickness of only 100 nm (Figure 4d and Table S1, Supporting Information). This demonstration bodes well for the prospect of using this electrode in high-performance OPVs of the future, because it is increasingly clear that for the large scale production of solution processed OPVs, the photoactive layer thickness will need to be increased to ≥300 nm,[22,23] because of the high defect density associated with much thinner bulk heterojunction (BHJ) layers together with the difficulty in achieving a uniform layer thickness over large areas using low cost printing methods. In this demonstrator OPV device, the nanowire network has been coated with a PEDOT:PSS layer, which is a widely used charge extraction layer for OPVs.[24–26] In this context, PH1000 spans the gaps in the Ag network and effectively collects charges whilst the Al4083 formulation optimizes the energetics at the electrode–semiconductor interface. The cross-section SEM image in Figure 4c shows the expected semicircular cross section of the Ag nanowires and that the network is conformally covered by the PEDOT:PSS layer.

3. Conclusions

This new concept in the fabrication of high-performance flexible transparent Ag nano-network electrodes addresses the drawbacks of complexity of the fabrication, instability of the

nanowire junctions, and high electrode surface roughness, which have limited the performance and utility of this type of electrode until now. The advantage of this unconventional approach is the simplicity, since there is no chemical or dry metal etching step, or mesh-transfer step. Additionally, the contact resistance between nanowires is zero and we show that the surface roughness is sufficiently low for integration into OPV devices with a photoactive layer thickness of only 100 nm, which bodes well for its utility in the future generation of OPVs which are expected to have much greater photoactive layer thickness. Given that electrospinning polymer NFs is compatible with roll-to-roll processing[27] and roll-to-roll vacuum evaporation of metals is proven as a low cost method of thin metal film deposition over large areas already widely used in the packaging industry, this new approach points the way to low cost continuous roll-to-roll fabrication of high-performance fused nanowire electrodes for myriad potential applications including organic electronics.

4. Experimental Section

Preparation of the Metal Repelling Layer: PFDMA (3 wt%) synthesized according to the literature[28] was dissolved in the fluorosolvent HFE-7500 (3M). Fifty microliters of FTS was added to the solution and stirred for 1 h. PET substrates were cleaned using acetone and IPA followed by a 30 min UV/O_3 treatment. The PFDMA:FTS blend was spin-coated onto UV/O_3 treated PET substrates at 1000 rpm for 30 s. The thickness of the PFDMA:FTS layer was ≈130 nm which was confirmed by AFM cross-section analysis.

Fabrication of Metal Nano-Networks: Three grams of PVP was dissolved in DMF:ethanol (2:8) to make an 8 wt% solution and stirred overnight to fully dissolve the polymer. APTMS and MPTMS (25 µL each) were added to the PVP solution and the blend was stirred for a further 4 h. This solution was loaded into a 5 mL syringe for electrospinning and electrospun onto the PET substrates coated with a 130 nm thick film of PFDMA:FTS. The voltage, flow rate, tip-substrate distance, relative humidity, needle gauge for the electrospinning process were 17 kV, 0.5 mL h^{-1}, 20 cm, 50%, and 25 G, respectively. The fiber collecting substrate was a metal plate (10 cm × 15 cm) covered with aluminium foil. PET substrates were placed onto the aluminium foil to get directly spun NFs. After the spinning samples were put into a crystallization dish with the lid covered and transferred into a fridge for 10 min at 5 °C, then they were exposed to atmosphere with 50% relative humidity for the fusion and flattening of the nano-fiber network. This can also be achieved by placing the samples into a desiccator with 1 mL of ethanol and reducing the pressure to 800 mbar for 10 min (see Supporting Information). The substrates were then transferred to the evaporation chamber for Ag deposition. The base pressure for the metal deposition was 2×10^{-6} mbar and the deposition rate for silver was 1 Å s^{-1}. After Ag deposition, the samples were gently rinsed in HFE-7500 for 10 s to remove the metal nanoparticles. In this study, all of the Ag nano-networks were solvent rinsed to remove the brown tinge unless otherwise stated. Notably, without the addition of FTS, this removal step is not possible (Figure S5, Supporting Information).

Measurements: The total and diffuse transmittance were measured using Lambda 1050 (PerkinElmer) equipped with an integral sphere. The PET (125 µm, Mitsubishi Polyester Film) substrate was used as a reference. The sheet resistance of ITO (Diamond Coatings Ltd., 15 Ω sq^{-1} sheet resistance with 80% transmittance at 550 nm wavelength) and nano-networks was measured by depositing silver pads to make a square electrode area.[29] PDMS substrates for stretch testing (60 µm-thick) and transferring the Ag nano-networks (7 mm-thick) were prepared from a Sylgard 184 kit with a base to curing agent ratio of 10:1 by weight. The mixture was poured onto FTS-treated silicon and cured at 100 °C for 4 h. The Ag nano-network was prepared on PDMS (60 µm) for stretching tests, and not rinsed using HFE-7500. The resistance change was measured according to the procedure given in ref. [30]. The morphology and current mapping of films were probed using an MFP-3D AFM (Asylum Research). The SEM images were obtained using ZEISS Gemini 500 (Gemini) and EDX spectra were recorded using an Oxford Instruments Si-Li detector unit on the SEM instrument with an accelerating voltage of 6 keV. The diameter of Ag nano-network lines was estimated using conventional DiameterJ and ImageJ software. The XPS analysis was performed using a Kratos AXIS Ultra DLD spectrometer and the data were analyzed using CasaXPS.

Calculation of Ag Condensation Coefficient (C): A 100 nm thick Ag film was evaporated onto an Si wafer (the reference substrate), and an Si wafer coated with PFDMA, PFDMA:FTS, and PVP NFs. EDX spectra were then collected from the same area size on each sample. The area underneath the Ag peak (2.77–3.08 keV) was determined for each sample (see Figure S12, Supporting Information). *C* was calculated by taking the ratio of the integrated area between the reference and the sample. Notably *C* is a function of deposited metal thickness.

Transparent Heaters: For transparent heaters, 2 cm × 2 cm and 4 cm × 4 cm PEN/ITO and PET/Ag nano-network samples were prepared. At either end of each substrate, a Cu strip was deposited by vacuum evaporation and Ag paste was applied to ensure a good electrical connection to the external circuit. Then DC voltage was applied using a Keithley 2400 sourcemeter and the temperature was measured using an infrared thermal imaging camera (FLIR i5). The heaters were suspended in air throughout the measurement.

Flexible OPV Fabrication: Flexible OPVs were fabricated with the following structure: PET/Ag nano-network/PH1000/Al4083/Bulk-heterojunction/PFN-Br/Al. Both PH1000 and PEDOT:PSS (Al4083) were modified with 6 vol% and 1 vol% ethylene glycol and HFE-7500, respectively, to improve the conductivity and wetting. The spin speeds for PH1000 and Al4083 were 2000 and 3000 rpm, respectively, and both films were annealed at 120 °C for 20 min, before transferring to a nitrogen-filled glove box for completion of the device. The bulk-heterojunction solution was prepared with PM6:Y6 (1:1, total 12 mg mL^{-1}) in chloroform and stirred for 2 h at 50 °C before the addition of 0.7 vol% 1-CN immediately prior to film deposition by spin-coating. The films were spun at 4500 rpm to achieve a bulk-heterojunction thickness of ≈100 nm and annealed at 80 °C for 10 min. PFN-Br was dissolved in methanol (0.5 mg mL) and spin-coated onto the bulk-heterojunction layer at 3500 rpm. Al was vacuum evaporated at 2×10^{-6} mbar through the pixel mask with 0.06 cm^2 area. The solar cell efficiency was measured in air without encapsulation under 1-sun simulated solar illumination and masked area of 0.0288 cm^2.

Supporting Information

Supporting Information is available from the Wiley Online Library or from the author.

Acknowledgements

This work was funded by United Kingdom Engineering and Physical Sciences Research Council (EPSRC) via grant number: EP/N009096/1 awarded to R.A.H. The authors thank Keun-Woo Park and Jin-Kyun Lee for synthesizing and supplying PFDMA and for commenting on the manuscript. All data supporting this study are provided as supplementary information accompanying this paper.

Conflict of Interest

The authors declare no conflict of interest.

Keywords

metal nanowires, nanofibers, selective deposition, transparent electrodes

Received: July 15, 2020
Revised: August 26, 2020
Published online:

[1] K. W. Seo, J. Lee, J. Jo, C. Cho, J. Y. Lee, *Adv. Mater.* **2019**, *31*, 1902447.
[2] H. Wu, D. Kong, Z. Ruan, P.-C. Hsu, S. Wang, Z. Yu, T. J. Carney, L. Hu, S. Fan, Y. Cui, *Nat. Nanotechnol.* **2013**, *8*, 421.
[3] T. He, A. Xie, D. H. Reneker, Y. Zhu, *ACS Nano* **2014**, *8*, 4782.
[4] K. Azuma, K. Sakajiri, H. Matsumoto, S. M. Kang, J. Watanabe, M. Tokita, *Mater. Lett.* **2014**, *115*, 187.
[5] P. C. Hsu, D. S. Kong, S. Wang, H. T. Wang, A. J. Welch, H. Wu, Y. Cui, *J. Am. Chem. Soc.* **2014**, *136*, 10593.
[6] J. Jang, B. G. Hyun, S. Ji, E. Cho, B. W. An, W. H. Cheong, J. U. Park, *NPG Asia Mater* **2017**, *9*, e432.
[7] J. Choi, Y. S. Shim, C. H. Park, H. Hwang, J. H. Kwack, D. J. Lee, Y. W. Park, B. K. Ju, *Small* **2018**, *14*, 1702567.
[8] X. D. Wang, Y. F. Zhang, X. J. Zhang, Z. H. Huo, X. Y. Li, M. L. Que, Z. C. Peng, H. Wang, C. F. Pan, *Adv. Mater.* **2018**, *30*, 1706738.
[9] S. B. Singh, Y. Hu, T. Kshetri, N. H. Kim, J. H. Lee, *J. Mater. Chem. C* **2017**, *5*, 4198.
[10] H. H. Khaligh, I. A. Goldthorpe, *Nanoscale Res. Lett.* **2013**, *8*, 235.
[11] S. Varagnolo, J. Lee, H. Amari, R. A. Hatton, *Mater. Hori.* **2019**, *7*, 143.
[12] H. M. Stec, R. J. Williams, T. S. Jones, R. A. Hatton, *Adv. Funct. Mater.* **2011**, *21*, 1709.
[13] J. Lee, M. Walker, S. Varagnolo, S. Huband, R. A. Hatton, *ACS Appl. Energy Mater.* **2019**, *2*, 5198.
[14] M. Akiba, A. S. Hashim, *Prog. Polym. Sci.* **1997**, *22*, 475.
[15] Y. G. Sun, Y. D. Yin, B. T. Mayers, T. Herricks, Y. N. Xia, *Chem. Mater.* **2002**, *14*, 4736.
[16] J. Lee, I. Lee, T. S. Kim, J. Y. Lee, *Small* **2013**, *9*, 2887.
[17] C. Sachse, N. Weiß, N. Gaponik, L. Müller-Meskamp, A. Eychmüller, K. Leo, *Adv. Energy Mater.* **2014**, *4*, 1300737.
[18] S. De, T. M. Higgins, P. E. Lyons, E. M. Doherty, P. N. Nirmalraj, W. J. Blau, J. J. Boland, J. N. Coleman, *ACS Nano* **2009**, *3*, 1767.
[19] S. Ji, W. He, K. Wang, Y. Ran, C. Ye, *Small* **2014**, *10*, 4951.
[20] W.-S. Cheong, Y.-H. Kim, J.-M. Lee, C.-H. Hong, H.-Y. Choi, Y.-J. Kwak, Y. J. Kim, Y. S. Kim, *Adv. Mater. Technol.* **2019**, *4*, 1800550.
[21] H. Lu, X. Ren, D. Ouyang, W. C. H. Choy, *Small* **2018**, *14*, 1703140.
[22] A. Armin, M. Hambsch, P. Wolfer, H. Jin, J. Li, Z. G. Shi, P. L. Burn, P. Meredith, *Adv. Energy Mater.* **2015**, *5*, 1401221.
[23] A. Armin, A. Yazmaciyan, M. Hambsch, J. Li, P. L. Burn, P. Meredith, *ACS Photonics* **2015**, *2*, 1745.
[24] C. Lee, D. J. Kang, H. Kang, T. Kim, J. Park, J. Lee, S. Yoo, B. J. Kim, *Adv. Energy Mater.* **2014**, *4*, 1301345.
[25] T. Lei, R. Peng, L. Huang, W. Song, T. Yan, L. Zhu, Z. Ge, *Mater. Today Energy* **2019**, *14*, 100334.
[26] W. Zhang, W. Song, J. Huang, L. Huang, T. Yan, J. Ge, R. Peng, Z. Ge, *J. Mater. Chem. A* **2019**, *7*, 22021.
[27] K. Chen, S. P. Nikam, Z. K. Zander, Y. H. Hsu, N. Z. Dreger, M. Cakmak, M. L. Becker, *ACS Appl. Polym. Mater.* **2020**, *2*, 304.
[28] S. H. Jung, K. Chuluunbandi, Y. Kim, J. Son, H. T. Oh, J. H. Lee, J. K. Lee, O. Beom-Hoan, *J. Polym. Sci. A Polym. Chem.* **2018**, *56*, 2672.
[29] J. Jin, J. Lee, S. Jeong, S. Yang, J. H. Ko, H. G. Im, S. W. Baek, J. Y. Lee, B. S. Bae, *Energy Environ. Sci.* **2013**, *6*, 1811.
[30] S. Hong, H. Lee, J. Lee, J. Kwon, S. Han, Y. D. Suh, H. Cho, J. Shin, J. Yeo, S. H. Ko, *Adv. Mater.* **2015**, *27*, 4744.